Frequency-Dependent Locally One-Dimensional FDTD Implementation With a Combined Dispersion Model for the Analysis of Surface Plasmon Waveguides

TAKAHASHI, Ryo / NAKANO, Hisamatsu / YAMAUCHI, Junji / SHIBAYAMA, Jun

(出版者 / Publisher)
IEEE

(雑誌名 / Journal or Publication Title)
IEEE Photonics Technology Letters / IEEE Photonics Technology Letters

(号 / Number)
10

(開始ページ / Start Page)
824

(終了ページ / End Page)
826

(発行年 / Year)
2008-05-15

Frequency-Dependent Locally One-Dimensional FDTD Implementation With a Combined Dispersion Model for the Analysis of Surface Plasmon Waveguides

Jun Shibayama, *Member, IEEE*, Ryo Takahashi, Junji Yamauchi, *Member, IEEE*, and Hisamatsu Nakano, *Fellow, IEEE*

***Abstract*—The implicit finite-difference time-domain (FDTD) method based on the locally one-dimensional scheme is extended to the frequency-dependent version for the analysis of the Drude–Lorentz model. The piecewise linear recursive convolution method is introduced, in which a large time step can be utilized. Analyses of a metal-cladding optical waveguide supporting a surface plasmon polariton reveal that the present method provides wavelength responses comparable to those of the explicit FDTD, while reducing the computational time to less than 50%.**

***Index Terms*—Locally one-dimensional finite-difference time-domain (LOD-FDTD) method, piecewise linear recursive convolution (PLRC) method, surface plasmon polariton (SPP).**

I. Introduction

METAL–insulator–metal-type optical waveguides supporting a surface plasmon polariton (SPP) have been extensively studied, since they allow light propagation in subwavelength structures [1]. For example, the frequency-dependent finite-difference time-domain (FDTD) method is used to analyze surface plasmon gratings formed by a periodic variation of the insulator width [2]. Note that to accurately analyze an SPP highly localized along a metal-insulator interface, spatial sampling widths must be extremely small. Unfortunately, this in turn leads to a small time step due to the Courant–Friedrich–Levy (CFL) condition [3], giving rise to long computational time.

To remove this restriction, the FDTD based on the alternating-direction implicit (ADI) scheme [4], [5] has been extended to the frequency-dependent version [6], [7]. Notice that the extension has been limited to single dispersion models, such as the Debye or Lorentz model. To accurately account for the frequency dispersion of the measured permittivity of a metal, the ADI-FDTD with the multispecies dispersion has recently been formulated [8] using the linear combination of the Drude and Lorentz models [9], [10]. This method uses the auxiliary differential equation (ADE) method [11].

On the other hand, we have proposed the efficient implicit FDTD based on the locally one-dimensional (LOD) scheme [12], [13], and formulated the frequency-dependent LOD-FDTD for the single dispersion model [14]. The main advantage of the LOD-FDTD is that the algorithm is quite simple with a concomitant reduction in computational time, while maintaining the accuracy comparable to the ADI-FDTD. This fact has recently motivated researchers to extend and improve the LOD-FDTD from several viewpoints [15]–[18].

In this work, we develop an efficient frequency-dependent LOD-FDTD method for the analysis of the Drude–Lorentz model. We introduce the piecewise linear recursive convolution (PLRC) method [19] that is generally efficient relative to the ADE method [14]. As an application, a metal-cladding (Au) optical waveguide is analyzed. We first investigate numerical accuracy of the recursive convolution (RC) and the PLRC methods. It is shown that the PLRC method retains high accuracy, even when a relatively large Δt is used. We next demonstrate the effectiveness of the PLRC-based LOD-FDTD through comparing the transmission spectrum and computational time with those from other methods.

II. Formulation

We consider the relative permittivity expressed by the following Drude–Lorentz model that gives a better fit of the dielectric function for Au and Ag, compared with the Drude model [9]:

$$\varepsilon_r(\omega) = \varepsilon_\infty + \frac{\omega_D^2}{j\omega\left(\nu_D + j\omega\right)} + \frac{\Delta\varepsilon_L\omega_L^2}{\left(j\omega\right)^2 + j\omega\nu_L + \omega_L^2} \quad (1)$$

where ε_∞ is the dielectric constant of the material at infinite frequency, ω is the angular frequency, ω_D and ω_L are the electron plasma frequencies, ν_D and ν_L are the effective electron collision frequencies, and $\Delta\varepsilon_L$ is the weighting coefficient for the Lorentz term. The subscripts D and L are used for the Drude and Lorentz models, respectively.

For dispersive media, the RC and PLRC methods are developed [19], in which the convolution can be efficiently performed. It is assumed that for the RC method the electric field is constant over Δt, while for the PLRC method the electric field has piecewise linear functional dependence over Δt. The accuracy of these two methods will be discussed later.

Application of the PLRC method with (1) to the LOD-FDTD for the TM wave results in

$$E_z^{n+1} = \frac{\varepsilon_\infty - \xi^0}{\varepsilon_\infty + \chi^0 - \xi^0}E_z^n + \frac{1}{\varepsilon_\infty + \chi^0 - \xi^0}\phi_z^n + \frac{\Delta t}{2\varepsilon_0\left(\varepsilon_\infty + \chi^0 - \xi^0\right)} \times \left(\frac{\partial H_y^{n+1/2}}{\partial x} + \frac{\partial H_y^n}{\partial x}\right) \quad (2a)$$

Manuscript received January 7, 2008; revised February 21, 2008. This work was supported in part by MEXT, Grant-in-Aid for Scientific Research (c) (19560355).

The authors are with the Faculty of Engineering, Hosei University, Tokyo 184-8584, Japan (e-mail: shiba@hosei.ac.jp).

Digital Object Identifier 10.1109/LPT.2008.921830

$$\frac{H_y^{n+1/2}-H_y^n}{\frac{\Delta t}{2}}=\frac{1}{\mu}\left(\frac{\partial E_z^{n+1}}{\partial x}+\frac{\partial E_z^n}{\partial x}\right) \tag{2b}$$

for the first step, where ε_0 is the permittivity of free space, μ is the permeability, $\chi^0=\chi_D^0+\mathrm{Re}(\chi_L^0)$, $\xi^0=\xi_D^0+\mathrm{Re}(\xi_L^0)$, and $\phi^n=\phi_D^n+\mathrm{Re}(\phi_L^n)$. ϕ_D^n and ϕ_L^n are expressed as

$$\phi_D^n=\left(\Delta\chi_D^0-\Delta\xi_D^0\right)E^n+\Delta\xi_D^0E^{n-1}+e^{-\nu_D\Delta t}\phi_D^{n-1}$$
$$\phi_L^n=\left(\Delta\chi_L^0-\Delta\xi_L^0\right)E^n+\Delta\xi_L^0E^{n-1}+e^{\gamma\Delta t}\phi_L^{n-1}$$

where $\gamma=-\alpha+j\beta$, $\alpha=\nu_L/2$, and $\beta=\sqrt{\omega_L^2-\alpha^2}$. χ_D^0, χ_L^0, $\Delta\chi_D^0$, and $\Delta\chi_L^0$ are given in [9]. ξ_D^0, ξ_L^0, $\Delta\xi_D^0$, and $\Delta\xi_L^0$ used for the PLRC formulation are derived as

$$\xi_D^0=\frac{\omega_D^2}{\nu_D}\left\{\frac{\Delta t}{2}-\frac{1}{\nu_D^2\Delta t}\left(1-e^{-\nu_D\Delta t}\right)+\frac{1}{\nu_D}e^{-\nu_D\Delta t}\right\}$$
$$\xi_L^0=-j\frac{\Delta\varepsilon_L\omega_L^2}{\gamma^2\beta\Delta t}\left\{(\gamma\Delta t-1)e^{\gamma\Delta t}+1\right\}$$
$$\Delta\xi_D^0=-\frac{\omega_D^2}{\nu_D^2}\left\{\frac{1}{\nu_D\Delta t}\left(1-e^{-\nu_D\Delta t}\right)^2-\left(1-e^{-\nu_D\Delta t}\right)e^{-\nu_D\Delta t}\right\}$$
$$\Delta\xi_L^0=\xi_L^0\left(1-e^{\gamma\Delta t}\right).$$

The equations for the second step can be obtained by the following changes to (2): $E_z\to E_x$, $\phi_z\to\phi_x$, $H_y^{n+1/2}\to H_y^{n+1}$, $H_y^n\to H_y^{n+1/2}$, $\partial/\partial x\to\partial/\partial z$, and $1/\mu\to-1/\mu$. When $\xi_{D,L}^0=0$ and $\Delta\xi_{D,L}^0=0$ are adopted, we obtain the equations for the RC method. In the first step, we substitute (2b) into (2a) and implicitly solve the resultant equation. Then, (2b) is explicitly solved. In the second step, the equations are calculated in the same way as in the first step. It should be noted that for the LOD-FDTD, two implicit and two explicit equations are solved. As a result, the number of explicit equations to be solved is reduced, when compared with the ADI counterpart in which two implicit and four explicit equations should be solved.

Note that in [9] the explicit FDTD with only the RC method is used to take into account (1). Here, although not shown, we newly formulate the explicit FDTD with the PLRC method for comparison with the LOD-FDTD results.

III. Numerical Results

We investigate the effectiveness of the LOD-FDTD through analyzing the optical waveguide shown in Fig. 1. The refractive index of the metal cladding (Au) is determined by (1) with the values of [9], i.e., for the Drude–Lorentz model $\varepsilon_\infty=5.9673$, $\omega_D/2\pi=2113.6$ THz, $\omega_L/2\pi=650.07$ THz, $\nu_D/2\pi=15.92$ THz, $\nu_L/2\pi=104.86$ THz, and $\Delta\varepsilon_L=1.09$ are used. For comparison, we examine the Drude model [9]: $\varepsilon_\infty=9.0685$, $\omega_D/2\pi=2155.6$ THz, and $\nu_D/2\pi=18.36$ THz. Due to the symmetry of the waveguide, only half the section $(x>0)$ is analyzed, in which the computational window size is $0.3\,\mu$m$\times 10\,\mu$m in the x and z directions, respectively. The sampling widths are $\Delta x=0.005\,\mu$m and $\Delta z=0.004\,\mu$m. The upper limit of the CFL condition is defined as Δt_{CFL} $(=0.00306$ fs), and the ratio of $\Delta t/\Delta t_{\mathrm{CFL}}$ as the CFL number (CFLN).

Unless otherwise stated, the TM pulse wave with a center wavelength of $0.7\,\mu$m is launched at the incidence plane (see Fig. 1), which consists of the eigenmode field in the x direction (confined to the air core region) and the Gaussian profile with a $1/e$ full-width of $1\,\mu$m in the z direction. The pulse is excited using the one-way excitation scheme, so that no field propagates toward the $-z$ direction. Since the computational window is large enough in the z direction, the calculation finishes before the pulse propagating in the $+z$ direction reaches the computational window edge. Therefore, no specific absorbing boundary condition is employed, i.e., fields are forced to zero at all computational window edges (using the perfectly matched layer [15], [16] is preferable for the analysis of more complex structures, which remains stable in our experiences with the present method). The wavelength characteristic of the transmission coefficient is calculated from the ratio between the discrete Fourier transforms of the incident pulse observed at #1 and the transmitted one at #2.

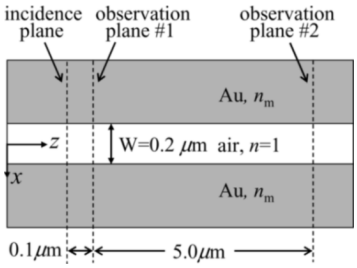

Fig. 1. Configuration of an optical waveguide with a metal (Au) cladding.

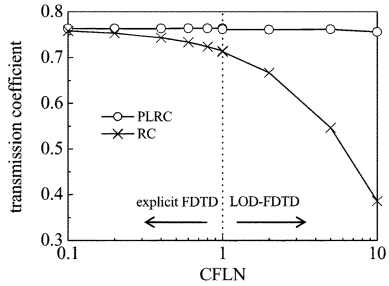

Fig. 2. Transmission coefficient at $\lambda=0.7\,\mu$m as a function of CFLN.

Since the accuracy of the RC and PLRC methods has not yet been fully understood in the optical waveguide analysis, we study it here with particular attention to the CFLN. Fig. 2 shows the transmission coefficient at a center wavelength of $\lambda=0.7\,\mu$m versus CFLN for the Drude–Lorentz model. Taking advantage of the unconditionally stable feature, we use the LOD-FDTD for $\mathrm{CFLN}\geq 1$. The data for $\mathrm{CFLN}\leq 1$ are obtained using the explicit FDTD. It is found that the accuracy of the PLRC method is retained, even when a large CFLN is used. Contrarily, the RC result gradually degrades with the CFLN. As a result, the PLRC method together with the implicit FDTD enables us to use a large CFLN.

Fig. 3 shows the wavelength response of the transmission coefficient using the LOD-FDTD. For comparison, also shown are the results obtained from the explicit FDTD with the continuous-wave excitation for a specific wavelength, and from the eigenmode solver (frequency-domain analysis) using the imaginary-distance implicit beam-propagation method based on Yee's mesh (YM-BPM) [20]. Note that the YM-BPM yields the propagation constant whose imaginary part corresponds to

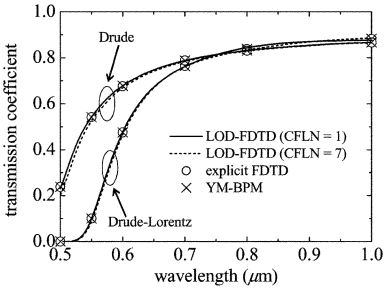

Fig. 3. Transmission characteristic as a function of wavelength.

an absorption coefficient or an attenuation constant α, which can readily be translated into the transmission coefficient of the waveguide ($\exp(\alpha l)$ where l is the waveguide length), and *vice versa*. It is clear that the results from the LOD-FDTD for $\mathrm{CFLN} = 1$ agree quite well with those from other methods, validating the present method (although not illustrated, the explicit FDTD curves with the pulse excitation are perfectly superimposed on the LOD-FDTD ones for $\mathrm{CFLN} = 1$). In addition, the LOD-FDTD for $\mathrm{CFLN} = 7$ is found to provide the acceptable numerical results.

Here, we mention the computational efficiency. The memory requirement of the LOD-FDTD (18.3 MB) is larger than that of the explicit FDTD (12.5MB), due to the implicit calculations. The computational time of the LOD-FDTD for $\mathrm{CFLN} = 1$ is 2.7 times as long as that of the explicit FDTD with the pulse excitation. Nevertheless, it is noteworthy that the time of the LOD-FDTD for $\mathrm{CFLN} = 7$ discussed above is reduced to $\simeq$39% of the explicit FDTD counterpart. The efficiency of the LOD-FDTD relative to the explicit FDTD somewhat depends on the size of the structure to be treated, e.g., for the extended waveguide twice as long as that analyzed previously the time for $\mathrm{CFLN} = 7$ is reduced to $\simeq$49%.

In Fig. 3, an appreciable difference can be seen between the Drude–Lorentz and Drude models in transmission coefficients for $\lambda < 0.7$ μm. When a waveguide with Au is analyzed for $\lambda < 0.7$ μm, we need to employ the permittivity determined from the Drude–Lorentz model that accurately accounts for the measured permittivity. This also becomes important for investigating a surface plasmon resonance sensor with Au used as a thin metal film, particularly when it operates in the visible wavelength region.

IV. Conclusion

The LOD-FDTD has been extended to the frequency-dependent version with a combined dispersion model. Although only the Drude–Lorentz model was considered, other combined dispersion models can similarly be treated. The PLRC method offers the use of a large time step allowed in the implicit FDTD, when compared with the RC method. It is demonstrated through the analysis of the metal-cladding optical waveguide that the computational time of the LOD-FDTD is reduced to less than 50% of that of the FDTD, while maintaining the comparable accuracy. The frequency-dependent LOD-FDTD can be extended to a three-dimensional problem [17], which will be left for a future study.

References

[1] K. Tanaka and M. Tanaka, "Simulations of nanometric optical circuits based on surface plasmon polariton gap waveguide," *Appl. Phys. Lett.*, vol. 82, no. 8, pp. 1158–1160, Feb. 2003.

[2] Z. Han, E. Forsberg, and S. He, "Surface plasmon Bragg gratings formed in metal-insulator-metal waveguides," *IEEE Photon. Technol. Lett.*, vol. 19, no. 2, pp. 91–93, Jan. 15, 2007.

[3] A. Taflove and S. C. Hagness, *Computational Electrodynamics: The Finite-Difference Time-Domain Method*. Norwood, MA: Artech House, 2000.

[4] T. Namiki, "A new FDTD algorithm based on alternating-direction implicit method," *IEEE Trans. Microw. Theory Tech* ., vol. 47, no. 10, pp. 2003–2007, Oct. 1999.

[5] F. H. Zheng, Z. Z. Chen, and J. Z. Zhang, "A finite-difference time-domain method without the Courant stability conditions," *IEEE Microw. Guided Wave Lett.*, vol. 9, no. 11, pp. 441–443, Nov. 1999.

[6] S. G. Garcia, R. G. Rubio, A. R. Bretones, and R. G. Martin, "Extension of the ADI-FDTD method to Debye media," *IEEE Trans. Antennas Propag.*, vol. 51, no. 11, pp. 3183–3186, Nov. 2003.

[7] S. W. Staker, C. L. Holloway, A. U. Bhobe, and M. P.-May, "Alternating-direction implicit (ADI) formulation of the finite-difference time-domain (FDTD) method: Algorithm and material dispersion implementation," *IEEE Trans. Electromagn. Compat.*, vol. 45, no. 2, pp. 156–166, May 2003.

[8] K.-Y. Jung and F. L. Teixeira, "Multispecies ADI-FDTD algorithm for nanoscale three-dimensional photonic metallic structures," *IEEE Photon. Technol. Lett.*, vol. 19, no. 8, pp. 586–588, Apr. 15, 2007.

[9] A. Vial, A.-S. Grimault, D. Macías, D. Barchiesi, and M. L. de la Chapelle, "Improved analytical fit of gold dispersion: Application to the modeling of extinction spectra with a finite-difference time-domain method," *Phys. Rev. B*, vol. 71, pp. 085416(1)–085416(7), Feb. 2005.

[10] T. Yamaguchi and T. Hinata, "Optical near-field analysis of spherical metals: Application of the FDTD method combined with the ADE method," *Opt. Express*, vol. 15, no. 18, pp. 11481–11491, Sep. 2007.

[11] T. Kashiwa and I. Fukai, "A treatment by FD-TD method of dispersive characteristics associated with electronic polarization," *Microw. Opt. Technol. Lett.*, vol. 3, no. 6, pp. 203–205, Jun. 1990.

[12] J. Shibayama, M. Muraki, J. Yamauchi, and H. Nakano, "Efficient implicit FDTD algorithm based on locally one-dimensional scheme," *Electron. Lett.*, vol. 41, no. 19, pp. 1046–1047, Sep. 2005.

[13] J. Shibayama, M. Muraki, R. Takahashi, J. Yamauchi, and H. Nakano, "Performance evaluation of several implicit FDTD methods for optical waveguide analyses," *J. Lightw. Technol.*, vol. 24, no. 6, pp. 2465–2472, Jun. 2006.

[14] J. Shibayama, R. Takahashi, J. Yamauchi, and H. Nakano, "Frequency-dependent LOD-FDTD implementations for dispersive media," *Electron. Lett.*, vol. 42, no. 19, pp. 1084–1086, Sep. 2006.

[15] V. E. d. Nascimento, B.-H. V. Borges, and F. L. Teixeira, "Split-field PML implementations for the unconditionally stable LOD-FDTD method," *IEEE Microw. Wireless Compon. Lett.*, vol. 16, no. 7, pp. 398–400, Jul. 2006.

[16] O. Ramadan, "Unsplit field implicit PML algorithm for complex envelope dispersive LOD-FDTD simulations," *Electron. Lett.*, vol. 43, no. 5, pp. 267–268, Mar. 2007.

[17] E. L. Tan, "Unconditionally stable LOD-FDTD method for 3-D Maxwell's equations," *IEEE Microw. Wireless Compon. Lett.*, vol. 17, no. 2, pp. 85–87, Feb. 2007.

[18] E. Li, I. Ahmed, and R. Vahldieck, "Numerical dispersion analysis with an improved LOD-FDTD method," *IEEE Microw. Wireless Compon. Lett.*, vol. 17, no. 5, pp. 319–321, May 2007.

[19] D. F. Kelly and R. J. Luebbers, "Piecewise linear recursive convolution for dispersive media using FDTD," *IEEE Trans. Antennas Propag.*, vol. 44, no. 6, pp. 792–797, Jun. 1996.

[20] J. Yamauchi, T. Mugita, and H. Nakano, "Implicit Yee-mesh-based finite-difference full-vectorial beam-propagation method," *J. Lightw. Technol.*, vol. 23, no. 5, pp. 1947–1955, May 2005.